1   **Future carbon emissions from global mangrove forest loss**

2   Adame, M.F.[1,2], R.M. Connolly[2], M.P. Turschwell[1], C.E. Lovelock[3], L. Fatoyinbo[4], D.

3   Lagomasino[5], L.A. Goldberg[6], J. Holdorf [2], D.A. Friess[7,8], SD. Sasmito[9,10], J. Sanderman[11],

4   M. Sievers[2], C. Buelow[2], B.J. Kauffman[12], D. Bryan-Brown[1], C.J. Brown[1, 2]

5

6   [1]Australian Rivers Institute, Griffith University, Nathan, 4111, QLD, Australia

7   [2]Australian Rivers Institute – Coast and Estuaries, School of Environment and Science, Griffith

8   University, Gold Coast, 4222, QLD, Australia

9   [3]School of Biological Sciences, The University of Queensland, St Lucia, 4072, Queensland,

10   Australia

11   [4]NASA Goddard Space Flight Center, Greenbelt, MD, USA

12   [5]Department of Coastal Studies, East Carolina University, Wanchese, NC, USA

13   [6]Earth System Science Interdisciplinary Center, University of Maryland, College Park, MD,

14   USA

15   [7]Department of Geography, National University of Singapore, 1 Arts Link, Singapore 117570

16   [8]Mangrove Specialist Group, International Union for Conservation of Nature (IUCN)

17   [9]Research Institute for Environment and Livelihoods, Charles Darwin University, Casuarina

18   0810, Australia

19   [10]Center for International Forestry Research, Bogor 16115, Indonesia

20   [11]Woods Hole Research Center. 149 Woods Hole Rd, Falmouth MA 02540, USA.

21   [12]Department of Fisheries, Wildlife and Conservation Sciences, Oregon State University,

22   Corvallis, OR 97331, USA

23

24

27   **Running head**: *Future carbon emissions from mangrove loss*

28

29

Abstract

Mangroves have among the highest carbon densities of any tropical forest. These "blue carbon" ecosystems can store large amounts of carbon for long periods, and their protection reduces greenhouse gas emissions and supports climate change mitigation. The incorporation of mangroves into Nationally Determined Contributions to the Paris Agreement and their valuation on carbon markets requires predicting how the management of different land-uses can prevent future greenhouse gas emissions and increase CO_2 sequestration. Management actions can reduce CO_2 emissions and enhance sequestration, but should be guided by predictions of future emissions, not just carbon storage. We project emissions and forgone soil carbon sequestration potential caused by mangrove loss with comprehensive global datasets for carbon stocks, mangrove distribution, deforestation rates, and drivers of land-use change. Emissions from mangrove loss could reach 2,397 Tg CO_{2eq} by the end of the century, or 3,401 Tg CO_{2eq} when considering forgone carbon sequestration. The highest emissions were predicted in southeast and south Asia (West Coral Triangle, Sunda Shelf, and the Bay of Bengal) due to conversion to aquaculture or agriculture, followed by the Caribbean (Tropical Northwest Atlantic) due to clearing and erosion, and the Andaman coast (West Myanmar) and north Brazil due to erosion. Together, these six regions accounted for 90% of the total potential CO_{2eq} future emissions. We highlight hotspots for future emissions and the land-use specfic management actions that could avoid them with appropriate policies and regulation.

Introduction

The capacity of mangroves to store carbon and mitigate greenhouse gas emissions became prominent a decade ago (Donato et al., 2011). Since then, mangroves have gained international interest for their potential to contribute to carbon mitigation strategies and for their ecosystem services that support adaptation to climate change (Lovelock & Duarte, 2019). Hundreds of site-scale studies have been conducted to understand the distribution and accumulation of mangrove soil carbon and aboveground biomass (Kauffman et al., 2020). These site-scale models have supported globally comprehensive spatial models of carbon storage (Rovai et al., 2018; Sanderman et al., 2018; Simard et al., 2019). Simultaneously, global efforts to accurately map and monitor mangrove cover and health have provided unprecedented knowledge on the risks that mangrove forests face (Bunting et al., 2018; Goldberg et al., 2020; Hamilton & Casey, 2016). These studies have enabled global-scale estimation of mangrove carbon storage and its historical loss across different nations (Murdiyarso et al., 2015; Serrano et al., 2019) and globally (Atwood et al., 2017).

Improved management can reduce CO_2 emissions from mangrove forest loss and enhance the sequestration potential of disturbed forests (Friess et al., 2020; O'Connor et al., 2020), but management actions should be guided by predictions of future emissions, not just carbon storage. The effectiveness of management relies on understanding how much emissions can be avoided by specific actions, for instance, by reducing land conversion or by increasing restoration efforts. Predictions of CO_2 emissions from mangrove loss linked with specific land-use changes can underpin the selection of actions to support adequate mangrove management actions for specific drivers of loss. These actions include improving the representation of mangroves in the National Determined Contributions (NDCs) committed to in the Paris Climate Agreement, strengthening their role as natural-based solutions, and improving their valuation on carbon markets (Adame et al., 2018; Seddon et al., 2019).

3

74   Recent advances in mapping of mangrove area, rates of loss, carbon storage and

75   emission factors now enable predictions of CO_2 emissions at the global scale (Worthington et

76   al., 2020). These predictions should overcome several key limitations in past studies

77   (Macreadie et al., 2019). First, carbon emission estimates have yet to associate particular

78   land-use changes with CO_2 emissions, as mapping of global drivers of mangrove loss has just

79   recently become available (Goldberg et al., 2020). Second, many global estimates have

80   included only the first meter of soil, thus, underestimating the total carbon content of

81   mangroves and the emissions that arise from their conversion to other land uses (Kauffman et

82   al., 2020). Third, estimates of global carbon emissions have not included the forgone carbon

83   sequestration and they do not account for the lost opportunity of sequestration when

84   mangroves are lost (Maxwell et al., 2019). And finally, global estimates have treated all CO_2

85   emissions from mangroves as occurring in the year of loss (Atwood et al., 2017). Depending

86   on the type of land-use change and the carbon pool affected, it can take years or even decades

87   for the carbon stored in mangroves to be emitted into the atmosphere (Lovelock et al., 2017)

88   and exported through tidal exchange (Maher et al., 2013).

89   To overcome current limitations in global estimations, we developed a spatial model

90   that projects emissions caused by mangrove loss. Our model synthesised information from

91   multiple newly available global datasets, including carbon stocks (Kauffman et al., 2020;

92   Sanderman et al., 2018; Simard et al., 2019), mangrove distribution (Bunting et al., 2018),

93   deforestation rates (Hamilton & Casey, 2016), drivers of land-use change (Goldberg et al.,

94   2020) and emissions factors (Sasmito et al., 2019). We provide predictions of future CO_2

95   emissions from mangrove loss, accounting for the effect of proximate drivers of land-use

96   change including: a) conversion to commodities, such as agriculture or aquaculture, b) coastal

97   erosion, c) clearing, d) extreme climatic events, and e) conversion to human settlements

98   (Goldberg et al., 2020). Importantly, we account for the foregone opportunity of soil carbon

99   sequestration when mangroves are lost (Maxwell et al., 2019). Our modelled emissions

100   reflect the realistic temporal scale of emissions, which are not annual, but decadal (Lovelock,

101   et al., 2017). By linking emissions with specific land-use changes and accounting for future

102   removals, we provide for the first time, spatially explicit information on how different drivers

103   of mangrove loss are causing CO_2 emissions and what management actions can prevent them.

104

Methods

<u>Mangrove area, rates of loss and drivers of change</u>

107   We divided global mangrove extent (Bunting et al., 2018) into the marine provinces (top-

108   level category of the bioregions) that contained mangroves (Spalding et al., 2007; Van der

109   Stocken et al., 2019; Fig. 1, S1, Table S1). We selected this approach to estimate global CO_2

110   emissions because it is well aligned with climatic and geomorphic characteristics of

111   mangroves, which are variables associated with carbon stocks and losses (Dürr et al., 2011;

112   Rogers et al., 2019). Deforestation rate for each province was obtained from the dataset by

113   Hamilton and Casey (2016) for the years 2000-2012.

114   The drivers of mangrove loss for each province (2000-2016) were obtained from

115   changes in mangrove area and a decision-tree model that separated drivers into five

116   categories: a) conversion to commodities, such as agriculture or aquaculture, b) coastal

117   erosion, c) clearing due to various activities including logging or hydrological modifications,

118   d) extreme climatic events, such as tropical storms and fluctuations in sea level, and e)

119   conversion to human settlements (Goldberg et al., 2020). Briefly, mangrove loss was

120   estimated from the Surface Reflectance Tier-1 Landsat 5TM, 7ETM+, and 8OLI imagery

121   within Google Earth Engine. A baseline period (1999-2001) of a Normalised Difference

122   Vegetation Index (NDVI) optimised mosaic representing the year 2000 was created from

5

123   where mangrove area change was estimated. A threshold change value of -0.2 that occurred

124   within the Mangrove Forests of the World extent (Giri et al., 2011) was used to indicate the

125   areas of mangroves that had transitioned from forest to no-forest (Lagomasino et al., 2019). A

126   random forest classification was applied to the areas showing a drop in NDVI greater than or

127   equal to 0.2. These areas were trained for each land cover type: water, dark soils, and bright

128   soils. Erosion was defined as a transition to water that intersected rivers and coastlines.

129   Commodities (agriculture/aquaculture) were defined where mangrove loss intersected the

130   Global Food Security-support Analysis Data Cropland Extent 30-m (GFSAD-30) layer

131   (www.usgs.gov/centers/wgsc/science/global-food-security-support-analysis-data-30-m).

132   Human settlements were defined as the bright soil land cover class that intersected with the

133   Global Human Settlements Layer (GHSL). Clearing or non-productive conversions were

134   defined at bright and dark soil land cover that intersected with a 5 km buffer around the

135   GRIP-4 global roads dataset (//doi.org/10.7927/H4VD6WCT) and the GHSL human

136   settlement dataset (//ghsl.jrc.ec.europa.eu/data.php). Lastly, conversion by extreme climatic

137   events was defined as all other areas of mangrove loss that did not occur within a 5 km

138   infrastructure buffer.

139   <u>Total Ecosystem Carbon Stocks (TECS)</u>

140   Soil organic carbon (SOC) stocks for one and two meters of soil were obtained from the

141   global SOC dataset (Sanderman et al., 2018), which was derived from a random forest model

142   trained on field measurements. For aboveground ecosystem carbon (ABC), biomass was

143   obtained from the global dataset of mangrove biomass (Simard et al., 2019). The total

144   biomass per province was divided by mangrove area to obtain a mean ABC per province and

145   multiplied by a factor of 0.48 to obtain carbon values (Kauffman & Donato, 2012). We

146   compared the TECS obtained from the global models with field measurements from

147   provinces where data was available (Kauffman et al., 2020) with a linear regression (IBM

6

148   SPSS Statistics, v25). TECS obtained from global models (Sanderman et al., 2018; Simard et

149   al., 2019) were lower in provinces with high stocks (> 1,200 MgC ha^{-1}, e.g. Sunda Shelf and

150   West Coral Triangle) and higher in provinces with small stocks (< 220 MgC ha^{-1}, e.g.

151   Northwest Australian Shelf and Somali Arabian). There were only 15 provinces with field

152   data, but the model predictions for these provinces were very close to the modelled data when

153   the depth of SOC was selected at two meters (Fig. S2, Table S1). Hence, we calculated TECS

154   for all provinces as the sum of ABC and SOC for the top two meters of soil.

155

156   Emissions factors

157   The emission factor is the fraction of carbon that is emitted given conversion to a specific

158   land-use. We selected an emission factor for each province and activity from a recent global

159   systematic review (Sasmito et al., 2019). Each emission factor was given a level of

160   confidence (Table S2) from low to high, with Level 1 (lowest confidence) given to emission

161   factors obtained from a global average, specific to that proximate driver; Level 2 to those

162   obtained from a similar region, specific to that proximate driver; and Level 3 (highest

163   confidence), from a similar region with the same geomorphic setting, specific to that

164   proximate driver (Dürr et al., 2011).

165

166   Model for projecting emissions and missed opportunities to sequester carbon

167   We updated a model of carbon emissions from deforested mangroves (Adame et al., 2018) to

168   account for drivers of land-uses and soil carbon sequestration. The model allowed for

169   variable carbon stocks across discrete spatial units and assumed a constant rate of

170   deforestation and a constant rate of emissions once mangroves were lost. We modelled

7

171   forgone carbon sequestration from mangrove loss in each province as the difference between

172   carbon storage with deforestation and a counterfactual with no deforestation:

173 $$L_t = C_t^0 - C_t^d \qquad (1)$$

174   Cumulative carbon emissions, L_t, were described by three dynamic equations:

175 $$\frac{dA}{dt} = -Ad \qquad (2)$$

176 $$\frac{dE}{dy} = A_1 \cdot d \cdot e^{-dt} \cdot c \cdot r \cdot e^{-(t-y)r} \qquad (3)$$

177 $$\frac{dS}{dt} = s \cdot A_1 e^{-dt} \qquad (4)$$

178   Where A is the area of mangroves in hectares, d is the total deforestation rate across

179   all land-uses, E is the emissions, r is the rate of emissions from deforested mangroves, c is the

180   total carbon stock emitted per hectare, y is the year of deforestation, S is sequestered carbon

181   and s is the yearly sequestration rate per hectare.

182   We assumed that future rates of deforestation due to each of the five drivers were in

183   proportion to their historical contributions to loss from Goldberg et al. (2020). Therefore,

184   province-specific potential emissions per hectare were scaled by land-use types and their

185   respective emission factors:

186 $$c_j = c_j^{max} \sum_{i=1}^{5} f_{i,j}\, p_{i,j} \qquad (5)$$

187   Where c_j^{max} is maximum labile carbon per hectare for a province including SOC and AGC,

188      $f_{i,j}$ are province and land-use specific emissions factors, and $p_{i,j}$ are the proportional contributions of

189   each land-use type to past deforestation.

190

191   *Sensitivity analyses to global datasets and model robustness*

192   To determine how sensitive our future predictions were to each of the variables

193   selected, we conducted sensitivity analyses where we repeated the predictions with different

194   datasets for mangrove area (Bunting et al., 2018; Hamilton & Casey, 2016), sources of data

195   (modelled and field) (Kauffman et al., 2020; Sanderman et al., 2018; Simard et al., 2019),

196   and SOC depth (1m, 2m, and whole sediment column).

197   We also conducted sensitivity analyses on the emissions factors relating to erosion

198   and extreme climatic events, which can be highly variable. Erosion can cause large emission

199   in one location but partly compensate the mangrove area loss by accretion in other areas

200   (Lagomasino et al., 2019). Extreme climatic events, such as tropical storms can cause large-

201   scale mortality; however, some areas can naturally recover after a few years if conditions are

202   appropriate, thereby reducing emissions (Krauss & Osland, 2020). Thus, we implemented the

203   model with emission factors of 50 and 100% for erosion, and with and without the mangrove

204   area loss from climatic events. Finally, we conducted further formal sensitivity analyses of

205   the model to all the parameter inputs by taking the derivative of L_t (cumulative carbon

206   emissions) with respect to each parameter.

207

Results and Discussion

209   *Inputs to the model*

210   First, we present summaries of the input data, noting that this data has been reported

211   elsewhere, but not aggregated by provinces. The mean TECS (mean ± SE, [range]) measured

212   in the field for all provinces was 624.5 ± 96.9 Mg C ha^{-1} (181.5–1,434.9). The mean

213   modelled SOC in the top meter of soil was 331.3 ± 74.9 (207.4–497.8) Mg C ha^{-1}, in the top

214   two meters was 646.7 ± 150.6 (408.6–975.9) Mg C ha^{-1}, and mean ABC was 101.2 ± 93.5

215   (9.9–466.0) Mg C ha^{-1}. The provinces with the largest area of mangroves were West Coral

216   Triangle, the Gulf of Guinea, Sahul Shelf, and Tropical Northwest Atlantic (Table S1, Fig.

217   S3). Ten provinces contained 88% of all the mangroves in the world. From 2000 to 2012, 35

218   of the 37 provinces had some level of deforestation, with mean annual losses of 0.09 ±

9

219   0.02%. The highest deforestation rates were in the Bay of Bengal (0.54%), Sunda Shelf (0.34

220   %), West Coral Triangle (0.32%), and Tropical Northwest Atlantic (0.14%) (Table S1, Fig.

221   S3).

222   Conversion of mangroves to aquaculture/agriculture was the primary proximate driver

223   of mangrove loss, which caused the conversion of 219,392 ha of mangroves from 2000 to

224   2016, especially in the West Coral Triangle (100,231 ha), Bay of Bengal (54,602 ha) and

225   Sunda Shelf (44,530 ha, Fig. 1A). This corresponds to 87.1, 73.5, and 70.4% of their total

226   mangrove loss, respectively. The second most important proximate driver of mangrove loss

227   was erosion, which caused the loss of 92,787 ha, mainly in North Brazil Shelf (20,547 ha,

228   54.9% of the total mangrove loss), the Bay of Bengal (14,309 ha, 19.3%) and Sunda Shelf

229   (11,863 ha, 18.8%). The third proximate driver of mangrove loss was extreme climatic

230   events, causing the loss of 41,525 ha of mangroves, mainly in North Brazil Shelf (8,605 ha,

231   5.7%), Tropical Northwest Atlantic (8,257 ha, 30.7%) and Sahul Shelf (8,480 ha, 42.2%).

232   The fourth most important driver was mangrove clearing which caused the loss of 39,595 ha,

233   mostly in Tropical Northwest Atlantic (9,244 ha, 30.7%), Gulf of Guinea (8,738 ha, 42.2%),

234   and West Indian Ocean (5,817 ha, 35.6%). Finally, the fifth proximate driver of mangrove

235   loss was human settlement, which caused the loss of 10,529 ha, mostly in the Sunda (3,980

236   ha, 6.3%) and Sahul Shelf (3,397 ha, 16.4%).

237

238   *Predictions of carbon emissions and lost opportunities to sequester carbons*

239   Global emissions from mangrove loss are projected to reach 2,397 $TgCO_{2\,eq}$ by the

240   end of the century (2020-2100). Including the loss of potential carbon sequestration once

241   mangroves are deforested (considered to have a global mean value of 1.5 MgC ha^{-1} yr^{-1};

242   Alongi, 2014) increased our projection to 3,401 $TgCO_{2\,eq}$. Previous estimates of mangrove

10

243   emissions for the same period varied enormously, between 630 and 40,230 $TgCO_{2eq}$ (Friess,

244   et al., 2020). Our projection lies towards the lower end of this range, and we consider it more

245   accurate because of the inclusion of land-use drivers, time lags, and foregone future

246   sequestration that were not considered in previous studies. Projected CO_2 emissions showed

247   significant geographical variability (Fig 1A). They were highest for the West Coral Triangle

248   (712 $TgCO_{2\ eq}$), followed by Sunda Shelf (452 $TgCO_{2\ eq}$), Bay of Bengal (369 $TgCO_{2\ eq}$),

249   Tropical Northwest Atlantic (312 $TgCO_{2\ eq}$), Andaman coast (161 $TgCO_{2\ eq}$), and North

250   Brazil Shelf (137 $TgCO_{2\ eq}$). Collectively, these provinces contributed 90% of the total

251   projected global CO_2 emissions (Fig. 1A, Fig. 2, Table S3).

252   The West Coral Triangle, Sunda Shelf, and the Bay of Bengal had the highest

253   predicted emissions due to mangrove conversion to agriculture/aquaculture at 985 $Tg\ CO_{2\ eq}$

254   (Fig. 1B, 2). This region has been previously highlighted as a global hotspot of mangrove

255   CO_2 emissions (Atwood et al., 2017). Within these provinces, clearing of large areas of

256   carbon-rich mangroves has occurred for rice, oil palm, aquaculture, and rubber plantations

257   (De Alban et al., 2019; Richards & Friess, 2016). In Indonesia, the conversion of mangroves

258   to aquaculture contributed almost 15% of their national emissions (Murdiyarso et al., 2015).

259   In Myanmar, deforestation of mangroves has been driven by national policies that support the

260   intensification of rice production to increase food security (Webb et al., 2014). Our

261   predictions suggest that emissions from the south and southeast East Asia will be the highest

262   globally by the end of the century due to the intensity of land-use changes and large

263   mangrove carbon stocks (Fig. S3). These emissions have the potential to be managed through

264   changes in agricultural practices, and the restoration of formerly converted mangrove areas,

265   such as disused aquaculture ponds and land with saltwater intrusion. For instance, the

266   improvement of the agriculture/aquaculture industry in the West Coral Triangle could reduce

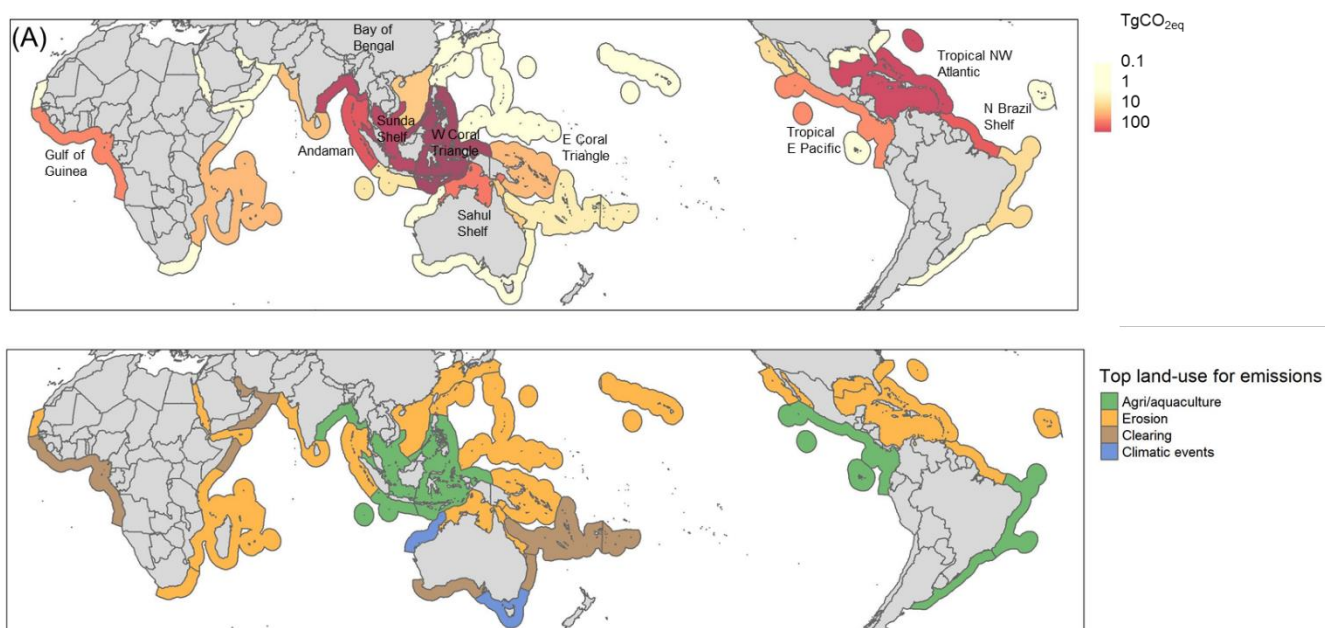267   up to 73% of the projected CO_2 emission for this region (Fig. 3A).

11

Figure. 1. (A) Global projected $CO_{2\,eq}$ emissions (Tg) by the end of the century (2010-2100) for the marine provinces of the world, and (B) the proximate driver responsible for the largest CO_2 emissions for each marine province (Goldberg et al. 2020). The names for all marine provinces can be found in Fig. S1 and Table S1.

An important driver of mangrove loss in the southeast and southeast Asia was erosion, which accounted for 23, 38, and 30% of the total emissions from the West Coral Triangle, Sunda Shelf, and Bay of Bengal provinces, respectively (Fig. 2). Additionally, the adjacent province of Andaman (west Myanmar, Bangladesh, and east India) had significant emissions due to erosion (98 $TgCO_{2\,eq}$ or 60% of its total emissions). In the Sundarbans, changes in river flows have reduced sediment inputs, which caused the loss of over 7,500 ha of coastline in the last 37 years (Bhargava et al., 2020). In areas prone to high rates of erosion, decreasing emissions would need to be achieved through shore stabilisation and the management of rivers and dams to provide sediment inputs that support the maintenance of mangrove surface elevations and habitat area (Lovelock et al., 2015; Fig. 3A). Landward migration of

284   mangroves, if coastal squeeze is avoided, may also balance some losses in provinces with

285   high levels of erosion (Schuerch et al., 2018).

286
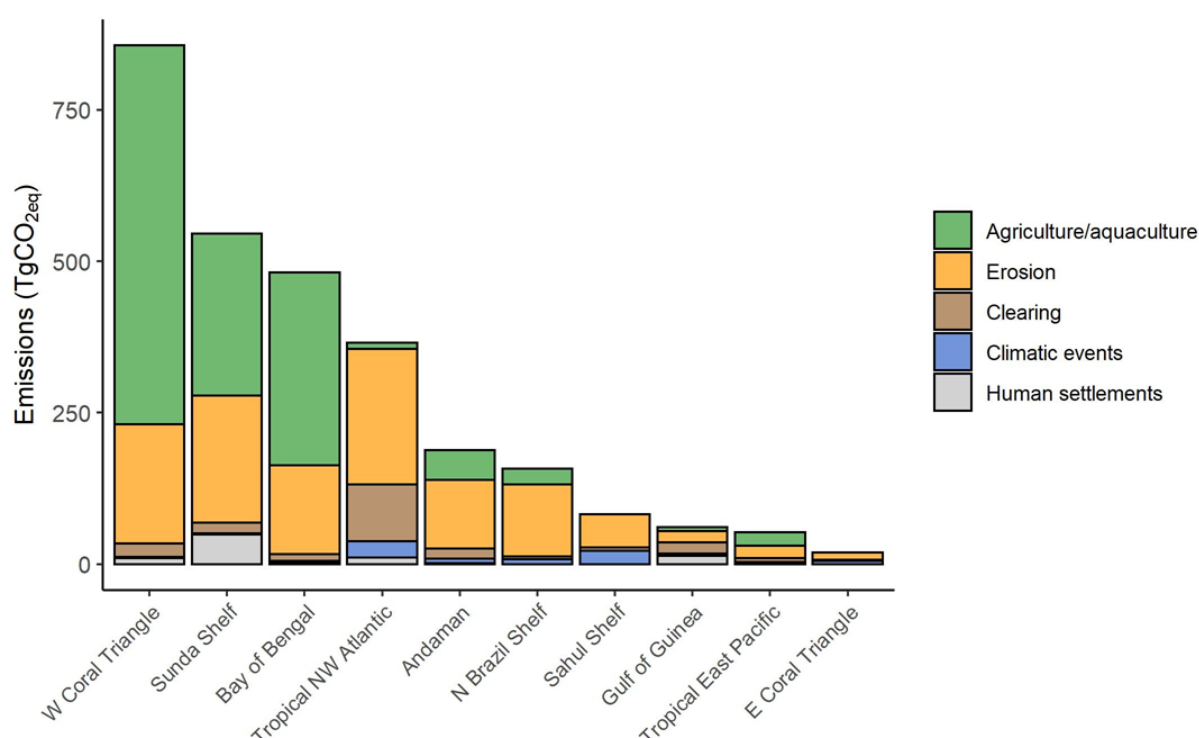
Figure 2. Cumulative $CO_{2\,eq}$ emissions (Tg) by the end of the century (2010-2100) attributed

288   to the proximate drivers of mangrove loss for the marine provinces ranked in the top ten for

289   future CO_2 emissions.

290

291   A second hotspot for mangrove CO_2 emissions was identified in the Tropical

292   Northwest Atlantic, which had large emissions due to erosion (191 $TgCO_{2\,eq}$), clearing (80

293    $TgCO_{2\,eq}$), and extreme climatic events (23 $TgCO_{2\,eq}$), with total emissions projected to reach

294   312 $TgCO_{2\,eq}$ by the end of the century (Fig. 1, 2; Table S2). In the Mexican Caribbean,

295   changes in hydrological connectivity that affect groundwater are a significant cause of

296   unintended clearing of mangroves that are rich in carbon (Adame et al., 2013). The Tropical

297   Northwest Atlantic is also one of the regions with the highest frequency of tropical storms in

13

298   the world, which can cause large-scale mangrove mortality (Krauss & Osland, 2020).

299   Management activities to decrease CO_2 emissions in the Tropical Northwest Atlantic could

300   include the stabilisation of the coasts, reduction of illegal deforestation and the improvement

301   of hydrological connectivity, especially in sites that fail to recover after tropical storms

302   (Zaldívar-Jiménez et al., 2010). These activities could reduce the projected carbon emissions
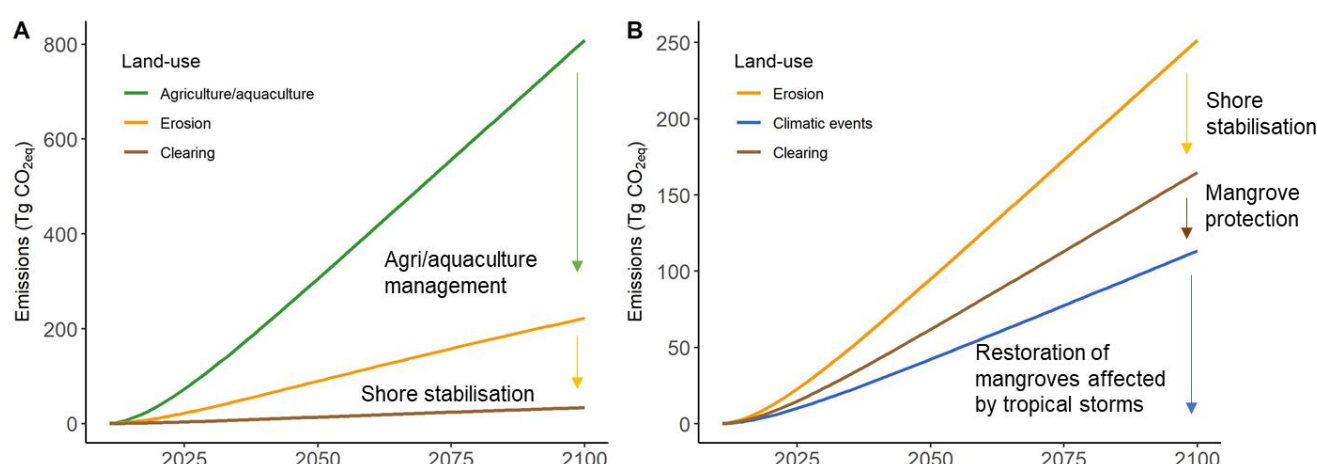
303   by 94% for this region (Fig. 3B).

304

305   **Figure 3.** Emission reductions (Tg CO_2 eq) that could be achieved from (A) management of

306   agriculture/aquaculture and shore stabilisation in the West Coral Triangle, and (B) decrease

307   in erosion through shore stabilisation, mangrove protection to avoid clearing, and

308   management of mangroves affected by tropical storms in the Tropical Northwest Atlantic.

309

310   Smaller hotspots with lower CO_2 emissions were predicted to occur on the North

311   Brazil Shelf, Sahul Shelf, and Gulf of Guinea (Fig. 1A), regions with an intermediate

312   mangrove area and moderate carbon stocks (Table S1). In Brazil, vegetation clearing,

313   changes in hydrology, and coastal development have increased erosion which has led to

314   mangrove loss (Krause & Soares, 2004). Across the Sahul Shelf, northern Australia, the loss

315   of mangroves during 2015-2016 was associated with an intense El Niño event which caused

14

316   fluctuating sea levels, drought, and high temperatures (Lovelock, et al., 2017). In the Gulf of

317   Guinea, CO_2 emissions are the result of drought and changes in hydrology, which caused the

318   loss of large areas of mangroves in Senegal (Sakho et al., 2017).

319

320   *Sensitivity of predictions to input data sources*

321   The sensitivity analysis demonstrated that our projected hotspots of CO_2 emissions

322   due to mangrove loss are robust to different input data for mangrove area, carbon stock and

323   emissions factors for extreme climatic events (Fig. S4). However, the total amount of

324   emissions from SOC and ABC varied when we considered modelled versus field data sets,

325   and different datasets for mangrove distribution (Fig S4). We considered field estimates to be

326   more accurate, and since estimates to 2 m were closer to field SOC measurements than the

327   estimates to 1 m (Fig. S2), we used 2 m as the depth of SOC for our predictions. Global

328   emissions predictions based on the mangrove distribution dataset of Global Mangrove Watch

329   (Bunting et al., 2018) were higher than those derived from the Hamilton and Casey (2016)

330   dataset (Fig. S4). The former is considered a more comprehensive representation of

331   mangrove forests globally because it captures mangroves of short stature. For instance, we

332   found that predictions in provinces where short-statured mangroves are dominant (e.g.

333   Tropical Northwest Atlantic) almost tripled when using the mangrove area from Global

334   Mangrove Watch (Bunting et al., 2018).

335   The sensitivity analysis also indicated the model was most sensitive to the

336   deforestation rates, with emissions increasing linearly as deforestation rate increased. The

337   model was also sensitive to emission rates, but only in the short-term (Fig. S5-S8). Therefore,

338   our model may overestimate emissions in regions where mangrove deforestation rates are

339   slowing because of policy changes (Friess, et al., 2020; Richards et al., 2020). We further

15

340   assumed that future rates of loss due to each of the five drivers were proportional to their

341   historical contributions. Therefore, if deforestation rates continue to slow into the future, our

342   CO_2 emissions predictions will be overestimated. Changes in the magnitude of all land-use

343   categories are likely to occur in the future, implying that our assumption of linearity in

344   predictions may not happen. For example, unused agricultural land may transition to urban

345   settlements. Also, mangrove loss may accelerate in some areas because of sea-level rise and

346   climatic events. In other areas, the expansion of mangroves onto floodplains could

347   compensate for some of the losses (Schuerch et al., 2018).

348   Overall our sensitivity analysis suggests that predictions on future emissions will be

349   most sensitive to deforestation rates; thus, a research priority is developing scenarios for

350   future mangrove loss that consider both climate and economic drivers of mangrove loss

351   (Duarte et al., 2020; Schuerch et al., 2018). Our CO_2 emission predictions could then be

352   updated to account for changes in land-use trajectories – and the resulting changes in losses

353   and gains – when higher-resolution global models of landscape change become available.

354

Conclusion

356   We have identified hotspots of CO_2 emissions due to mangrove loss associated with

357   various drivers of land-use change. We predict that emissions arising from mangrove loss

358   within this century will be concentrated in six provinces of the world: West Coral Triangle,

359   Sunda Shelf, Bay of Bengal, Tropical Northwest Atlantic, Andaman, and North Brazil Shelf.

360   These regions have large areas of mangroves (> 500,000 ha), relatively high rates of loss ($\geq$

361   0.1 % annually), and most of them have high carbon densities ($\geq$ 500 MgC ha^{-1}). By

362   accounting for specific land-use changes and the foregone carbon sequestration potential, we

363   update previous global estimates and provide specific management actions to most efficiently

16

364   minimise future emissions. Activities that improve agricultural practices to reduce further

365   expansion into mangrove areas, and efforts to stabilise coastlines and restore former

366   mangrove areas should be prioritised to decrease emissions from mangrove loss by the end of

367   the century.

Acknowledgements

Authors Contributions

MFA, RMC, CJB designed the project with major contributions from DF and CL; CJB, MT, and JH, designed the codes and models: LF, DL and LG, provided spatial data and analyses of mangrove loss drivers, JS provided spatial data and analyses of soil carbon, BK provided field data, SDF and DF provided data on emission factors; MS and DB conducted spatial analyses. MFA wrote the first draft and all authors contributed to editing subsequent drafts.

Supplementary Material is available for this paper.

Data availability

Data will be fully available at the Griffith University Data Repository and the repository of the Center for International Forestry Research (CIFOR).

Correspondence and requests for materials should be addressed to f.adame@griffith.edu.au

18

References

394

395 Adame, Brown, C. J., Bejarano, M., Herrera-Silveira, J. A., Ezcurra, P., Kauffman, J. B., &
396   Birdsey, R. (2018). The undervalued contribution of mangrove protection in Mexico to
397   carbon emission targets. *Conservation Letters*, *11*(4), e12445.
398   https://doi.org/10.1111/conl.12445

399 Adame, M. F., Kauffman, J. B., Medina, I., Gamboa, J. N., Torres, O., Caamal, J. P., Reza,
400   M., & Herrera-Silveira, J. a. (2013). Carbon stocks of tropical coastal wetlands within
401   the karstic landscape of the Mexican Caribbean. *PLoS ONE*, *8*(2), e56569.
402   https://doi.org/10.1371/journal.pone.0056569

403 Alongi, D. M. (2014). Carbon cycling and storage in mangrove forests. *Annu. Rev. Mar. Sci*,
404   *6*, 195–219. https://doi.org/10.1146/annurev-marine-010213-135020

405 Atwood, T. B., Connolly, R. M., Almahasheer, H., Carnell, P. E., Duarte, C. M., Ewers
406   Lewis, C. J., Irigoien, X., Kelleway, J. J., Lavery, P. S., Macreadie, P. I., Serrano, O.,
407   Sanders, C. J., Santos, I., Steven, A. D. L., & Lovelock, C. E. (2017). Global patterns in
408   mangrove soil carbon stocks and losses. *Nature Climate Change*, *7*(June), 523–528.
409   https://doi.org/10.1038/nclimate3326

410 Bhargava, R., Sarkar, D., & Friess, D. (2020). A cloud computing-based approach to
411   mapping mangrove erosion and progradation: case studies from the Sundarbans and
412   French Guiana. *Estuarine, Coastal and Shelf Science*. doi: 10.1016/j.ecss.2020.106798

413 Bunting, P., Rosenqvist, A., Lucas, R. M., Rebelo, L. M., Hilarides, L., Thomas, N., Hardy,
414   A., Itoh, T., Shimada, M., & Finlayson, C. M. (2018). The global mangrove watch - A
415   new 2010 global baseline of mangrove extent. *Remote Sensing*, *10*(10), 1669.
416   https://doi.org/10.3390/rs10101669

417 De Alban, J. D. T., Jamaludin, J., Wong, D. de W., Than, M. M., & Webb, E. L. (2019).
418   Improved estimates of mangrove cover and change reveal catastrophic deforestation in
419   Myanmar. *Environmental Research Letters*. https://doi.org/10.1088/1748-9326/ab666d

420 Donato, D. C., Kauffman, J. B., Murdiyarso, D., Kurnianto, S., Stidham, M., & Kanninen, M.
421   (2011). Mangroves among the most carbon-rich forests in the tropics. *Nature
422   Geoscience*, *4*, 293–297.

423 Duarte, C. M., Agusti, S., Barbier, E., Britten, G. L., Castilla, J. C., Gattuso, J. P., Fulweiler,
424   R. W., Hughes, T. P., Knowlton, N., Lovelock, C. E., Lotze, H. K., Predragovic, M.,
425   Poloczanska, E., Roberts, C., & Worm, B. (2020). Rebuilding marine life. *Nature*,
426   *580*(7801), 39–51. https://doi.org/10.1038/s41586-020-2146-7

427 Dürr, H. H., Laruelle, G. G., van Kempen, C. M., Slomp, C. P., Meybeck, M., & Middelkoop,
428   H. (2011). Worldwide typology of nearshore coastal systems: Defining the estuarine
429   filter of river inputs to the oceans. *Estuaries and Coasts*, *34*(3), 441–458.
430   https://doi.org/10.1007/s12237-011-9381-y

431 Friess, D., Krauss, K. W., Taillardat, P., Adame, M., Yando, E. S., Cameron, C., Sasmito, S.,
432   & Meriadec, S. (2020). Mangrove blue carbon in the face of deforestation, climate
433   change and restoration. *Annual Plant Reviews*, In press.

434 Friess, D., Yando, E. S., Abuchahla, G. M. O., Adams, J. B., Cannicci, S., Canty, S. W. J.,
435   Cavanaugh, K. C., Connolly, R. M., Cormier, N., Dahdouh-Guebas, F., Diele, K., Feller,

I. C., Fratini, S., Jennerjahn, T. C., Lee, S. Y., Ogurcak, D. E., Ouyang, X., Rogers, K., Rowntree, J. K., … Wee, A. K. S. (2020). Mangroves give cause for conservation optimism, for now. *Current Biology*, *30*(4), R153–R154. https://doi.org/10.1016/j.cub.2019.12.054

Giri, C., Ochieng, E., Tieszen, L. L., Zhu, Z., Singh, a., Loveland, T., Masek, J., & Duke, N. (2011). Status and distribution of mangrove forests of the world using earth observation satellite data. *Global Ecology and Biogeography*, *20*(1), 154–159. https://doi.org/10.1111/j.1466-8238.2010.00584.x

Goldberg, L., Lagomasino, D., Thomas, N., & Fatoyinbo, T. (2020). Global declines in human-driven mangrove loss. *Global Change Biology*, *March*, 1–12. https://doi.org/10.1111/gcb.15275

Hamilton, S. E., & Casey, D. (2016). Creation of a high spatio-temporal resolution global database of continuous mangrove forest cover for the 21st century (CGMFC-21). *Global Ecology and Biogeography*, *25*(6), 729–738. https://doi.org/10.1111/geb.12449

Kauffman, J., Adame, M. F., Arifanti, V. B., Schile-Beers, L. M., Bernardino, A. F., Bhomia, R. K., Donato, D. C., Feller, I. C., Ferreira, T. O., Jesus Garcia, M. del C., MacKenzie, R. A., Megonigal, J. P., Murdiyarso, D., Simpson, L., & Hernández Trejo, H. (2020). Total ecosystem carbon stocks of mangroves across broad global environmental and physical gradients. *Ecological Monographs*, *90*(2), e01405. https://doi.org/10.1002/ecm.1405

Kauffman, J. B., & Donato, D. C. (2012). *Protocols for the measurement, monitoring and reporting of structure, biomass and carbon stocks in mangrove forests. Working paper 86.*

Krause, G., & Soares, C. (2004). Analysis of beach morphodynamics on the Bragantinian mangrove peninsula (Pará, North Brazil) as pre requisite for coastal zone management recommendations. *Geomorphology*, *60*, 225–239.

Krauss, K. W., & Osland, M. J. (2020). Tropical cyclones and the organisation of mangrove forests: a review. *Annals of Botany*, *125*, 213–234. https://doi.org/10.1093/aob/mcz161

Lagomasino, D., Fatoyinbo, T., Lee, S., Feliciano, E., Trettin, C., Shapiro, A., & Mangora, M. (2019). Measuring mangrove carbon loss and gain in deltas. *Environmental Research Letters*, *14*(2), 025002.

Lovelock, C. E., Cahoon, D. R., Friess, D. A., Guntenspergen, G. R., Krauss, K. W., Reef, R., Rogers, K., Saunders, M. L., Sidik, F., Swales, A., Saintilan, N., Thuyen, L. X., & Triet, T. (2015). The vulnerability of Indo-Pacific mangrove forests to sea-level rise. *Nature*, *526*(7574), 559–563. https://doi.org/10.1038/nature15538

Lovelock, C. E., & Duarte, C. M. (2019). Dimensions of blue carbon and emerging perspectives. *Biology Letters*, *15*(3). https://doi.org/10.1098/rsbl.2018.0781

Lovelock, C. E., Feller, I. C., Reef, R., Hickey, S., & Ball, M. C. (2017). Mangrove dieback during fluctuating sea levels. *Scientific Reports*, *7*(1), 1–8. https://doi.org/10.1038/s41598-017-01927-6

Lovelock, C. E., Fourqurean, J. W., & Morris, J. T. (2017). Modeled CO2 emissions from coastal wetland transitions to other land uses: tidal marshes, mangrove forests, and seagrass beds. *Frontiers in Marine Science*, *4*. https://doi.org/10.3389/fmars.2017.00143

479 Macreadie, P. I., Anton, A., Raven, J. A., Beaumont, N., Connolly, R. M., Friess, D. A.,
480   Kelleway, J. J., Kennedy, H., Kuwae, T., Lavery, P. S., Lovelock, C. E., Smale, D. A.,
481   Apostolaki, E. T., Atwood, T. B., Baldock, J., Bianchi, T. S., Chmura, G. L., Eyre, B.
482   D., Fourqurean, J. W., … Duarte, C. M. (2019). The future of Blue Carbon science.
483   *Nature Communications*, *10*(1), 1–13. https://doi.org/10.1038/s41467-019-11693-w

484 Maher, D. T., Santos, I. R., Golsby-Smith, L., Gleeson, J., & Eyre, B. D. (2013).
485   Groundwater-derived dissolved inorganic and organic carbon exports from a mangrove
486   tidal creek: The missing mangrove carbon sink? *Limnology and Oceanography*, *58*(2),
487   475–488. https://doi.org/10.4319/lo.2013.58.2.0475

488 Maxwell, S. L., Evans, T., Watson, J. E. M., Morel, A., Grantham, H., Duncan, A., Harris,
489   N., Potapov, P., Runting, R. K., Venter, O., Wang, S., & Malhi, Y. (2019). Degradation
490   and forgone removals increase the carbon impact of intact forest loss by 626%. *Science
491   Advances*, *5*(10). https://doi.org/10.1126/sciadv.aax2546

492 Murdiyarso, D., Purbopuspito, J., Kauffman, J. B., Warren, M. W., Sasmito, S. D., Donato,
493   D. C., Manuri, S., Krisnawati, H., Taberima, S., & Kurnianto, S. (2015). The potential of
494   Indonesian mangrove forests for global climate change mitigation. *Nature Climate
495   Change*, *5*, 1089–1092. https://doi.org/10.1038/nclimate2734

496 O'Connor, J., Fest, B., Sievers, M., & Swearer, S. (2020). Impacts of land management
497   practices on blue carbon stocks and greenhouse gas fluxes in coastal ecosystems—A
498   meta-analysis. *Global Change Biology*, *26*(3), 1354–1366.

499 Richards, D. R., & Friess, D. A. (2016). Rates and drivers of mangrove deforestation in
500   Southeast Asia, 2000–2012. *Proceedings of the National Academy of Sciences*, *113*(2),
501   344–349. https://doi.org/10.1073/pnas.1510272113

502 Richards, D. R., Thompson, B. S., & Wijedasa, L. (2020). Quantifying net loss of global
503   mangrove carbon stocks from 20 years of land cover change. *Nature Communications*,
504   *11*, 4260. https://doi.org/10.1038/s41467-020-18118-z

505 Rogers, K., Kelleway, J. J., Saintilan, N., Megonigal, J. P., Adams, J. B., Holmquist, J. R.,
506   Lu, M., Schile-Beers, L., Zawadzki, A., Mazumder, D., & Woodroffe, C. D. (2019).
507   Wetland carbon storage controlled by millennial-scale variation in relative sea-level rise.
508   *Nature*, *567*(7746), 91–95. https://doi.org/10.1038/s41586-019-0951-7

509 Rovai, A. S., Twilley, R. R., Castañeda-Moya, E., Riul, P., Cifuentes-Jara, M., Manrow-
510   Villalobos, M., Horta, P. A., Simonassi, J. C., Fonseca, A. L., & Pagliosa, P. R. (2018).
511   Global controls on carbon storage in mangrove soils. *Nature Climate Change*, *8*(6),
512   534–538. https://doi.org/10.1038/s41558-018-0162-5

513 Sakho, I., Dupont, J. P., Cisse, M. T., El Janyani, S., & Loum, S. (2017). Hydrological
514   responses to rainfall variability and dam construction: a case study of the upper Senegal
515   River basin. *Environmental Earth Sciences*, *76*, 253.

516 Sanderman, J., Hengl, T., Fiske, G., Solvik, K., Adame, M. F., Benson, L., Bukoski, J. J.,
517   Carnell, P., Cifuentes-Jara, M., Donato, D., Duncan, C., Eid, E. M., Ermgassen, P. Z.,
518   Lewis, C. J. E., Macreadie, P. I., Glass, L., Gress, S., Jardine, S. L., Jones, T. G., …
519   Landis, E. (2018). A global map of mangrove forest soil carbon at 30 m spatial
520   resolution. *Environmental Research Letters*, *13*, 055002. https://doi.org/10.1088/1748-
521   9326/aabe1c

522 Sasmito, S. D., Taillardat, P., Clendenning, J. N., Cameron, C., Friess, D. A., Murdiyarso, D.,

21

523   & Hutley, L. B. (2019). Effect of land-use and land-cover change on mangrove blue
524   carbon: A systematic review. *Global Change Biology*, *25*(12), 4291–4302.
525   https://doi.org/10.1111/gcb.14774

526   Schuerch, M., Spencer, T., Temmerman, S., Kirwan, M. L., Wolff, C., Lincke, D., McOwen,
527   C. J., Pickering, M. D., Reef, R., Vafeidis, A. T., Hinkel, J., Nicholls, R. J., & Brown, S.
528   (2018). Future response of global coastal wetlands to sea-level rise. *Nature*, *561*(7722),
529   231–234. https://doi.org/10.1038/s41586-018-0476-5

530   Seddon, N., Sengupta, S., Hauler, I., & Rizvi, A. R. (2019). *Nature-based Solutions in*
531   *Nationally Determined Contributions: synthesis and recommendations for enhancing*
532   *climate ambition and action by 2020.*

533   Serrano, O., Lovelock, C. E., B. Atwood, T., Macreadie, P. I., Canto, R., Phinn, S., Arias-
534   Ortiz, A., Bai, L., Baldock, J., Bedulli, C., Carnell, P., Connolly, R. M., Donaldson, P.,
535   Esteban, A., Ewers Lewis, C. J., Eyre, B. D., Hayes, M. A., Horwitz, P., Hutley, L. B.,
536   … Duarte, C. M. (2019). Australian vegetated coastal ecosystems as global hotspots for
537   climate change mitigation. *Nature Communications*, *10*(1).
538   https://doi.org/10.1038/s41467-019-12176-8

539   Simard, M., Fatoyinbo, L., Smetanka, C., Rivera-Monroy, V. H., Castañeda-Moya, E.,
540   Thomas, N., & Van der Stocken, T. (2019). Mangrove canopy height globally related to
541   precipitation, temperature and cyclone frequency. *Nature Geoscience*, *12*(1), 40–45.
542   https://doi.org/10.1038/s41561-018-0279-1

543   Spalding, M. D., Fox, H. E., Allen, G. R., Davidson, N., Ferdaña, Z. A., Finlayson, M. A. X.,
544   Halpern, B. S., Jorge, M. A., Lombana, A. L., Lourie, S. A., Martin, K. D., Manus, M.
545   C., Molnar, J., Recchia, C. A., & Robertson, J. (2007). Marine Ecoregions of the World :
546   A bioregionalisation of coastal and shelf areas. *BioScience*, *57*(7), 573–583.

547   Van der Stocken, T., Carroll, D., Menemenlis, D., Simard, M., & Koedam, N. (2019).
548   Global-scale dispersal and connectivity in mangroves. *Proceedings of the National*
549   *Academy of Sciences of the United States of America*, *116*(3), 915–922.
550   https://doi.org/10.1073/pnas.1812470116

551   Webb, E. L., Jachowski, N. R. A., Phelps, J., Friess, D. A., Than, M. M., & Ziegler, A. D.
552   (2014). Deforestation in the Ayeyarwady Delta and the conservation implications of an
553   internationally-engaged Myanmar. *Global Environmental Change*, *24*(1), 321–333.
554   https://doi.org/10.1016/j.gloenvcha.2013.10.007

555   Worthington, T. A., Andradi-Brown, D. A., Bhargava, R., Buelow, C., Bunting, P., Duncan,
556   C., Fatoyinbo, L., Friess, D. A., Goldberg, L., Hilarides, L., Lagomasino, D., Landis, E.,
557   Longley-Wood, K., Lovelock, C. E., Murray, N. J., Narayan, S., Rosenqvist, A., Sievers,
558   M., Simard, M., … Spalding, M. (2020). Harnessing big data to support the conservation
559   and rehabilitation of mangrove forests globally. *One Earth*, *2*(5), 429–443.
560   https://doi.org/10.1016/j.oneear.2020.04.018

561   Zaldívar-Jiménez, M. A., Herrera-Silveira, J. A., Teutli-Hernández, C., Comín, F. A.,
562   Andrade, J. L., Molina, C. C., & Ceballos, R. P. (2010). Conceptual framework for
563   mangrove restoration in the Yucatán Peninsula. *Ecological Restoration*, *28*(3), 333–342.
564   https://doi.org/10.3368/er.28.3.333

565